Reliability of the double-folding potential for fusion cross sections of light systems

Azni Abdul Aziz,[1,2,3,*] Norhasliza Yusof,[1,2] Muhammad Zamrun Firihu,[4,†] and Hasan Abu Kassim[1,2,5]

[1]*Department of Physics, Faculty of Science, University of Malaya, 50603 Kuala Lumpur, Malaysia*

[2]*Quantum Science Center, Department of Physics, Faculty of Science, University of Malaya, 50603 Kuala Lumpur, Malaysia*

[3]*Kulliyah of Science, International Islamic University Malaysia, 25200 Kuantan, Pahang, Malaysia*

[4]*Department of Physics, Halu Oleo University, Kendari, 93232 Sulawesi Tenggara, Indonesia*

[5]*Institute of Space Science, Universiti Kebangsaan Malaysia, 43600 Bangi, Selangor, Malaysia*

(Received 6 July 2014; revised manuscript received 2 October 2014; published 29 January 2015)

We study the fusion reaction of light systems with one-dimensional barrier penetration model using the α-α double-folding cluster (DFC) potential. We especially analyze the fusion cross sections of the $^{12}C + ^{12}C$, ^{16}O, ^{24}Mg, ^{28}Si, $^{16}O + ^{16}O$, $^{24}Mg + ^{24}Mg$, ^{28}Si, and $^{28}Si + ^{28}Si$ reactions. The results are compared with the one obtained with M3Y double folding (DFM) and the Akyüz-Winther (A-W) potentials. It is found that the calculations with DFM and DFC potentials can reproduce the experimental data much better than the calculations using the A-W potential. We also carried out an analysis on the astrophysical aspect of the $^{12}C + ^{12}C$, ^{16}O, and $^{16}O + ^{16}O$ reactions. The calculations using DFC and DFM potentials could fit the S-factor data reasonably well. However, the calculated reaction rates are lower than the compilation of Caughlan and Fowler at low temperatures. In the important range of temperatures in stellar evolution, the DFC potential reproduces very satisfactory fitting to the experimental cross section and the S-factor data and gives a consistent prediction of astrophysical reaction rates. This finding indicates that the DFC potential could be used as an alternative potential to study the fusion reactions in the astrophysical interest.

DOI: 10.1103/PhysRevC.91.015811 PACS number(s): 25.70.Jj, 24.10.Ht, 26.20.−f

I. INTRODUCTION

For over more than four decades, heavy-ion fusion reactions have been studied extensively. The basic approach to the heavy-ion fusion reactions, which is based on the one-dimensional barrier penetration model, has been successful in describing the experimental fusion cross sections at energies above the Coulomb barrier [1,2]. However, it is found that this model fails to explain the enhancement of the fusion cross section at energies below the Coulomb barrier, which is called the sub-barrier fusion reaction. It is now well established that this enhancement can be explained by the coupled-channel formalism and it is widely utilized for low-energy heavy-ion fusion reactions [1,3–5].

The nuclear interaction between the projectile and the target nuclei with the mass number A_P and A_T, respectively, within their distance of closest approach, r, is described by the Woods-Saxon shaped potential and is given by [6]

$$V_N(r) = \frac{-V_0}{1+\exp[(r-R_0)/a_0]} + i\frac{-W_0}{1+\exp[(r-R_W)/a_W]}, \quad (1)$$

where $R_0 = r_0(A_P^{1/3} + A_T^{1/3})$ and $R_W = r_W(A_P^{1/3} + A_T^{1/3})$. The real part is characterized by the surface diffuseness parameter, a_0, the potential depth, V_0, and the radius parameter, r_0, which can be obtained using the Akyüz-Winther parametrization [6]. This potential is usually called the Akyüz-Winther (A-W) potential. The a_W, W_0, and r_W are the surface diffuseness parameter, the potential depth, and the radius parameter for the imaginary part, respectively, but the values are not necessarily to be the same as for the real part.

It was noted that the usage of the Woods-Saxon shaped potential has not been possible to simultaneously reproduce different reaction observable, such as fusion [7], elastic scattering [8,9], and quasielastic scattering [10–12]. Another current inadequacy of understanding the nuclear potential is the fusion hindrance where the measurements of fusion cross sections below the $\sim$100 μb level exhibit a behavior that is different from the coupled-channel predictions [13]. A much steeper falloff was observed at extreme sub-barrier energies for heavy and medium systems [14]. For light heavy-ion systems, this effect is not well established since the experimental data of the fusion cross sections are still not low enough to confirm its existence [15,16].

Due to the importance in the detailed understanding of the nuclear potential, various models have been developed to analyze the experimental data. In the past three decades, the double folding model [8,17–19] has been widely used in describing the heavy-ion scattering, due to its simple handling in numerical calculations. Further developments in improving the model for obtaining a better description of the experimental data is done by using the M3Y effective nucleon-nucleon (NN) interaction in the calculations. Up to now, several versions of the double folding with M3Y interaction (DFM) have been proposed [20].

Apart from that, another type of double folding potential, based on α-α interaction folded with the α-cluster distributions in the colliding nuclei, has been described by Azab *et al.* [21]. A nucleus of mass number A is considered to be the composed of an integral number, m of α particles, i.e., $A = 4m$. This type of potential is known as the α-α double-folding cluster (DFC) potential. Several studies using this potential

*Corresponding author: azni_abdulaziz@yahoo.com

†Corresponding author: mzamrun@yahoo.com

have been conducted by emphasizing elastic scattering [21,22]. The studies reported that this model can successfully explain the differential cross section of elastic scattering data for a few reactions. Recently, a study by Kocak *et al.* [23] has also shown that this potential could describe the broad features of the fusion, the S factor, and the elastic scattering angular data, simultaneously.

Therefore, in this paper, we concentrate on the investigation of the DFC potential behavior, specifically on fusion. We would like to see how well it could reproduce the fusion experimental data compared to the DFM and the A-W potentials for light systems with $A \leqslant 28$, i.e., the $^{12}C + ^{12}C$, ^{16}O, ^{24}Mg, ^{28}Si, $^{16}O + ^{16}O$, $^{24}Mg + ^{24}Mg$, ^{28}Si, and $^{28}Si + ^{28}Si$ reactions. Since the reactions of $^{12}C + ^{12}C$, ^{16}O, and $^{16}O + ^{16}O$ systems are important in stellar carbon and oxygen burnings, the investigation on the astrophysical aspect will also be carried out.

The paper is organized as follows. In the next section, we briefly explain the main formula used for DFM and DFC potentials. The results of the calculations are presented in the Sec. III for fusion cross sections and in Sec. IV for the astrophysical aspect of the fusion reactions. We summarize the paper in Sec. V.

II. THE FORMALISM

The interaction potential between two nuclei is written as

$$U(R) = U_C(R) + U_n(R) + U_{\rm rot}(R), \tag{2}$$

where U_C is the Coulomb interaction, U_n is the nuclear interaction, and $U_{\rm rot}$ is the rotational term. The Coulomb interaction and the rotational term are well known. However, the nuclear part of the interaction is less defined. In this work, the real part of the nuclear interaction is calculated using two different double-folding potentials, i.e., the DFC and DFM potentials. In practice, the strength of the double-folding potential has often been renormalized by a certain factor to give the best fit to the experimental scattering data. This factor is attributed to the higher-order terms, which cannot be easily calculated.

Although a detailed description for both potentials can be found in many references [18–21,23], the main formula is presented in this paper in order to clearly differentiate the interaction used for both potentials. Details of both calculations are discussed below.

A. M3Y double-folding model potential

The nuclear part of this potential, $V_{\rm DFM}$, consists of two terms: the direct term, $V_{\rm DFMD}$, and the exchange term, $V_{\rm DFME}$, which are in general energy dependent. The direct part of the interaction between two colliding nuclei is given by

$$V_{\rm DFMD}(R, E_p) = g(E_P) \int d\vec{r}_P \int d\vec{r}_T \rho_{PA}(\vec{r}_P) \upsilon_D(\vec{s}) \rho_{TA}(\vec{r}_T), \tag{3}$$

where ρ_{PA} and ρ_{TA} are the nucleon densities of the colliding nuclei, while $g(E_P) = 1 - kE_P$ is a multiplier that depends upon the energy per nucleon $E_P = E_{\rm lab}/A_P$. The direct part of the nuclear interaction, υ_D, which depends on the relative position of the interacting nuclei, $\vec{s}$, is given by the M3Y effective nucleon-nucleon interaction,

$$\upsilon_D(s) = \sum_{i=1}^{3} G_{Di}[\exp(-s/r_{vi})]/(s/r_{vi}). \tag{4}$$

It is determined by the radius parameter, r_{vi}, and the coefficient, G_{Di}, where the values are given by either Reid or Paris interactions as given in Table I.

TABLE I. The coefficients of the Reid and Paris M3Y interactions [20].

Coefficients	Reid	Paris
G_{D1} (MeV)	7999	11062
G_{D2} (MeV)	−2134	−2537.5
G_{D3} (MeV)	0	0
r_{v1} (fm)	0.25	0.25
r_{v2} (fm)	0.40	0.40
r_{v3} (fm)	1.414	1.414
$G_{E\delta}$ (MeV fm^3)	−276	−592
k (MeV^{-1})	0.002	0.003

Current development on the double-folding potential in order to obtain a better description of the elastic scattering data has lead to the introduction of the realistic density dependent for the effective NN interaction and the explicit treatment of the exchange potential using a realistic local approximation. In general, the calculation of the exchange potential is quite complicated due to its nonlocality. To avoid explicit treatment of the nonlocality in the calculation of the exchange potential, a simple zero-range exchange (ZE) pseudopotential is still widely used instead of the finite-range exchange. Therefore, in order to make a direct comparison with the DFC potential, the DFM potential with density-independent of zero-range exchange for M3Y-Reid interaction has been chosen, which is given by $\upsilon_{E\delta}(\vec{s}) = G_{E\delta}\delta(\vec{s})$. By using this type of exchange interaction, one can easily evaluate the potential by only replacing $\upsilon_D(\vec{s})$ with $\upsilon_{E\delta}(\vec{s})$ in the integral of Eq. (3).

The density distribution for both the projectile and the target nuclei is given by the two-parameter Fermi (2pF) formula [24]

$$\rho_{P(T)Z}(r) = \rho_{0P(T)}\{1 + \exp[(r - R_{P(T)})/a_{P(T)}]\}^{-1}, \tag{5}$$

where the nucleon density is taken to be proportional to the proton density: $\rho_{P(T)A} = \rho_{P(T)Z}A/Z$ and ρ_0 arises from the normalization process. The parameters $R_{P(T)}$ and $a_{P(T)}$ are defined using the electron elastic scattering data from Table 1 of Ref. [24]. The radius parameters for the nucleon and proton densities are taken to be equal to those for the charge density, whereas the diffuseness parameters are corrected for the finite width of the charge distribution of a single proton, which can be calculated via the equation [8]

$$a_Z^2 = a_{\rm ch}^2 - \frac{5}{7\pi^2}\left(\langle r_{1p}^2\rangle + \langle r_{1n}^2\rangle \frac{N}{Z}\right). \tag{6}$$

Here $\langle r_{1p}^2\rangle$ (msrp) and $\langle r_{1n}^2\rangle$ (msrn) are the mean-square radii of the proton and neutron charge distributions, respectively.

B. The α-α double-folding cluster model potential

The DFC potential is constructed in a way similar to the ordinary DFM potential. The only differences are in the treatment of the nucleon-nucleon interaction and the nuclear matter density. In the DFC potential, the folded α-α effective interaction with α-cluster distribution densities is formulated as

$$V_{\mathrm{DFC}}(\vec{r}) = \iint \rho_{cP}(\vec{r}_P)\rho_{cT}(\vec{r}_T)\upsilon_{\alpha\alpha}(\vec{s})d\vec{r}_T d\vec{r}_P. \quad (7)$$

The vector $\vec{s} = |\vec{R} + \vec{r}_T - \vec{r}_P|$ while ρ_{cP} and ρ_{cT} are the α-cluster distributions for the projectile and target nuclei and $\upsilon_{\alpha\alpha}$ is the effective α-α interaction. The α-α potential considered in this calculation is taken from Buck *et al.* [25], since it is the most favorable and simplest potential available, and is given by

$$\upsilon_{\alpha\alpha} = -122.6225\exp(-0.22r^2). \quad (8)$$

The matter density distribution of both the projectile and the target nuclei can be written as

$$\rho_M(\vec{r}) = \rho_{0M}(1 + \omega r^2)\exp(-\beta r^2), \quad (9)$$

which is a modified form of the Gaussian shape, while the corresponding α density is

$$\rho_\alpha(\vec{r}) = \rho_{0\alpha}\exp(-\lambda r^2). \quad (10)$$

If ρ_c is the α-cluster distribution function inside the nucleus, then the nuclear matter density distribution function of the nucleus, ρ_M, can be related to that of the α-particle nucleus, ρ_α, as

$$\rho_M(\vec{r}) = \int \rho_c(\vec{r'})\rho_\alpha(|\vec{r} - \vec{r'}|)d\vec{r'}. \quad (11)$$

The densities of the nucleus and the α particle can be calculated from Eqs. (9) and (10) by using the Fourier transform on Eq. (11) [8]. Thus, the α-cluster distribution function ρ_c is obtained as

$$\rho_c(\vec{r'}) = \rho_{0c}(1 + \mu r'^2)\exp(-\xi r'^2) \quad (12)$$

with

$$\eta = \lambda - \beta, \quad \xi = \beta\lambda/\eta, \quad \mu = \frac{2\omega\lambda^2}{\eta(2\eta - 3\omega)},$$
$$\rho_{0c} = \frac{A}{4}\sqrt{\frac{\xi^3}{\pi^3}}\frac{2\xi}{2\xi + 3\mu}. \quad (13)$$

All the important parameters for the nuclei considered in this study are given in Table II.

TABLE II. The nuclear density parameters.

Nucleus	ρ_0 (fm^{-3})	ω (fm^{-2})	$\beta(\lambda)$ (fm^{-2})	$\langle r^2\rangle^{1/2}$ (fm)	Ref.
^{4}He	0.4229	0	0.7024	1.461	[8]
^{12}C	0.1644	0.4988	0.3741	2.407	[26]
^{16}O	0.1317	0.6457	0.3228	2.640	[26]
^{24}Mg	0.1499	0.4012	0.2383	3.050	[22]
^{28}Si	0.2050	0.1941	0.2112	3.140	[27]

III. FUSION CROSS SECTION

In this work, the fusion cross section is calculated with one-dimensional barrier penetration model by using the DFM and DFC potential to replace the real part of the nuclear interaction in Eq. (1). The nuclear interaction is then written as

$$U_N(r) = N_R V_{\mathrm{DFC}(M)}(r) + i\frac{-W_0}{1 + \exp[(r - R_W)/a_W]}. \quad (14)$$

The normalization factor, N_R, is varied in order to optimize the fit to the experimental data. The best fit could be obtained by minimizing the χ^2/N value, where N is the number of data points.

The imaginary potential parameters considered in this calculation are energy independent. The values are taken to be $W_0 = 50$ MeV, $r_W = 1.0$ fm, and $a_W = 0.4$ fm. These are chosen in order to simulate the compound nucleus formation. The calculated fusion cross section is insensitive to these parameters as long as it is strong enough and well localized inside the Coulomb barrier. This is to make sure that any differences arise only from the real part of the potential.

The double-folding potentials are calculated using the CCODE [28], which is designed to calculate the nucleus-nucleus interaction energy for two spherical nuclei. Since the potential is calculated using the Fourier transform, the α-α potential considered in DFC potential has been transformed into the k-space configuration:

$$\upsilon_{\alpha\alpha}(k) = -122.6225\sqrt{\frac{\pi^3}{0.010648}}\exp\left(\frac{-k^2}{0.88}\right). \quad (15)$$

In this work, the Reid interaction of zero-range exchange NN interaction is chosen for the calculation of DFM and the details of the calculation have been described in Refs. [20] and [28]. The nuclear potentials of DFM and DFC are then fed into the CCQEL code [29] to calculate the cross section for some selected reactions. The cross section calculated using DFM

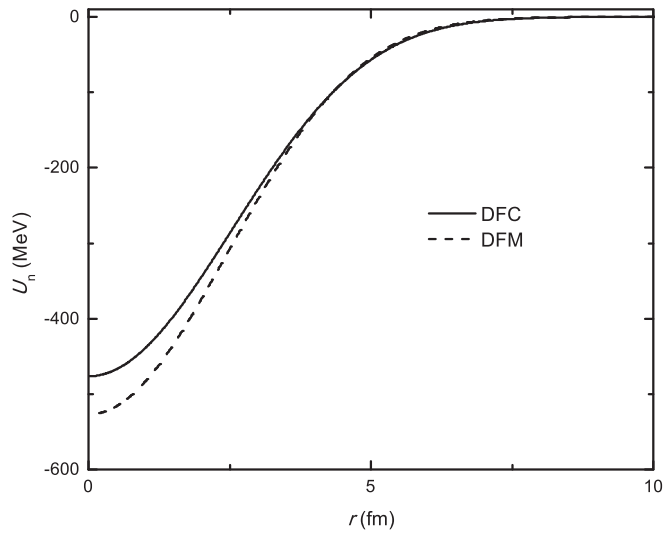

FIG. 1. The nuclear potentials obtained with DFM (dashed line) and DFC (solid line) potentials, respectively, for the $^{16}O + ^{16}O$ reaction.

and DFC potentials are then compared to the cross section obtained with the A-W potential.

The result shows that DFC and DFM potentials produce very deep potentials, as demonstrated in Fig. 1. The DFC potential seems to be less attractive compared to the DFM potential. The potential can be calculated using Eq. (2). It is found that the barrier height produced by DFC potential is always lower than DFM potential (see Table III). As an example, we showed in Fig. 2 the total potential for the ^{24}Mg + ^{24}Mg reaction. In order to illustrate the difference between double folding and A-W potentials, we plot in Fig. 3 the barrier height, B, and the percentage of fractional difference, Diff = $100(B_{\mathrm{DFM}(C)} - B_{A-W})/(B_{A-W})$ versus $B_Z = Z_P Z_T/(A_P^{1/3} + A_T^{1/3})$ MeV.

TABLE III. The barrier height, B, and position, R_B, obtained using A-W, DFM, and DFC potentials, respectively, for the reactions considered in this paper. The corresponding value of χ^2 fitting is also listed.

Reaction	Potential	N_R	B	R_B	χ^2	B_Z
^{12}C + ^{12}C						7.86
	A-W		6.13	7.82	54.17	
	DFM	1.00	6.32	7.58	50.82	
		1.45	6.13	7.85	52.93	
	DFC	1.00	6.20	7.79	42.83	
		1.17	6.13	7.89	59.41	
^{12}C + ^{16}O						9.98
	A-W		7.97	8.02	2.03	
	DFM	1.00	8.12	7.87	5.42	
		1.27	7.97	8.04	2.13	
	DFC	1.00	8.02	8.03	2.52	
		1.09	7.97	8.09	2.00	
^{16}O + ^{16}O						12.70
	A-W		10.03	8.53	1.63	
	DFM	1.00	10.47	8.14	10.79	
		1.72	10.03	8.55	1.67	
	DFC	1.00	10.38	8.26	6.98	
		1.35	10.16	8.48	1.42	
^{12}C + ^{24}Mg						13.92
	A-W		11.52	8.33	6.63	
	DFM	1.00	11.52	8.31	4.45	
	DFC	1.00	11.34	8.50	13.13	
		0.82	11.52	8.34	4.43	
^{12}C + ^{28}Si						15.77
	A-W		13.24	8.47	31.96	
	DFM	1.00	13.38	8.37	20.12	
	DFC	1.00	13.00	8.63	49.93	
		0.78	13.27	8.42	21.53	
^{24}Mg + ^{24}Mg						24.96
	A-W		21.76	8.83	4.59	
	DFM	1.00	21.32	8.98	20.54	
		0.788	21.76	8.76	3.95	
	DFC	1.00	21.03	9.14	50.39	
		0.66	21.77	8.76	4.00	
^{24}Mg + ^{28}Si						28.37
	A-W		25.03	8.96	15.54	
	DFM	1.00	24.75	9.03	29.27	
		0.875	25.03	8.91	13.83	
	DFC	1.00	24.19	9.26	165.14	
		0.67	25.03	8.87	13.04	
^{28}Si + ^{28}Si						32.27
	A-W		28.81	9.09	18.90	
	DFM	1.00	28.74	9.08	19.56	
		0.97	28.81	9.06	16.20	
	DFC	1.00	27.85	9.37	157.02	
		0.677	28.81	8.98	12.03	

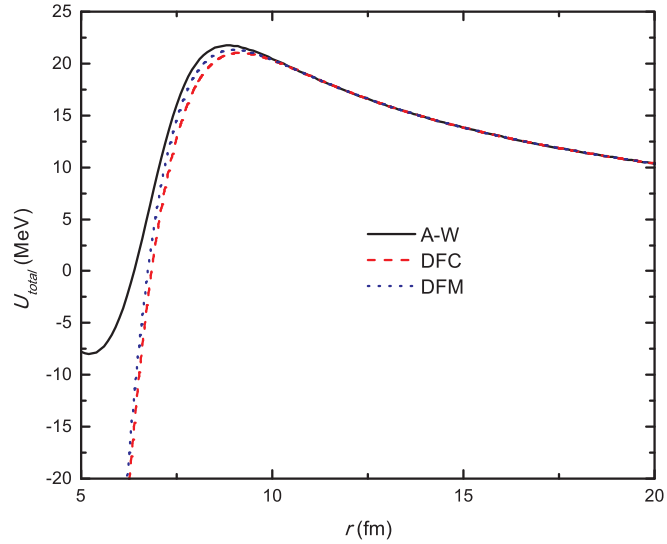

FIG. 2. (Color online) Comparison of total potential obtained with DFM (thick-dotted line), DFC (dashed line), and A-W (solid line) potentials, respectively, for ^{24}Mg + ^{24}Mg reaction.

The fusion cross sections calculated from the double folding potentials underestimated the experimental data for ^{12}C + ^{16}O and ^{16}O + ^{16}O reactions. However, for the rest of the reactions, they give higher values than the measured cross sections. In order to fit the experimental data then the renormalization constants are required. It is found that the constants are greater than unity for the ^{12}C + ^{16}O and ^{16}O + ^{16}O reactions, and for the other the reactions, the constants are around 0.66–0.97. The details are listed in Table III.

It seems that the DFM potential could give the best fit to the ^{12}C + ^{24}Mg and ^{12}C + ^{28}Si reactions with no adjustment on the potential strength. The best fitting for both double-folding potentials could be obtained if the strength of the potentials is adjusted in such a way that the barrier height is similar to that calculated from A-W potential. This explains the similar trend of the renormalization constant with the difference in the barrier height between the double-folding and the A-W potentials as plotted in Fig. 3. However, for the ^{12}C + ^{12}C reaction, although the barrier heights obtained from both double-folding potentials are higher than the A-W potential, they could produce the best fitting without renormalization. Overall, both double-folding potentials with the adjustment on the potential strength could reproduce the fusion cross section better than the A-W potential.

IV. ASTROPHYSICAL ASPECTS

The heavy-ion reactions involving ^{12}C and ^{16}O nuclei play an important role in the behavior of highly developed stars.

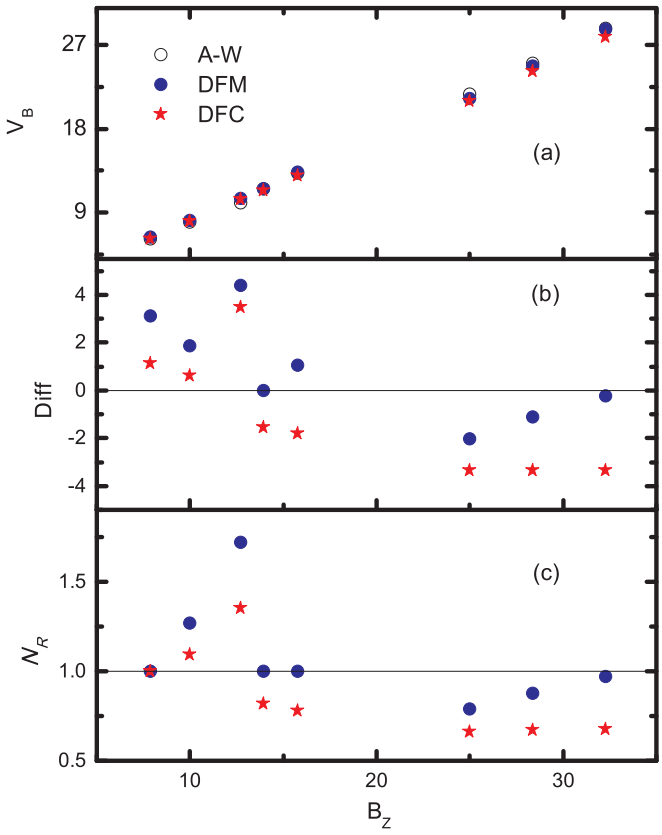

FIG. 3. (Color online) (a) The calculated fusion barrier energies of DFM (solid circle) and DFC (solid star) potentials in comparison with the one obtained by using A-W potential (open circle) as a function of B_Z. (b) The percentage differences between DFM and A-W potentials (solid circle) and between DFC and A-W potentials (solid star). (c) The normalization constant, N_R, gives the best fit to the experimental fusion cross section for the calculations by using DFM (solid circle) and DFC (solid star) potentials, respectively.

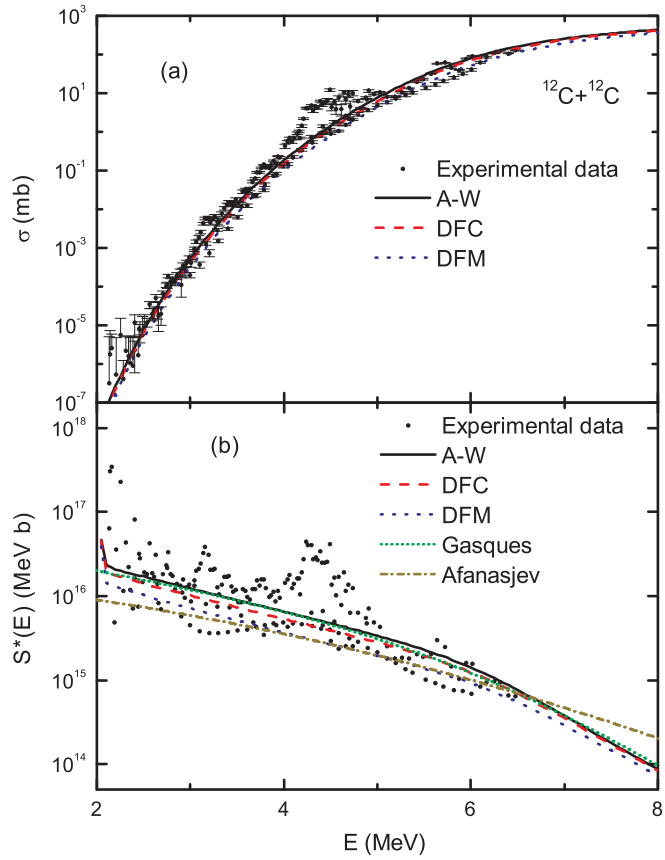

FIG. 4. (Color online) The calculated (a) cross section and (b) modified astrophysical S factor for $^{12}C + ^{12}C$ reaction. The solid and the dashed lines are the results of the calculations using the A-W and the DFC potentials, respectively. The thick dotted line is obtained using the DFM potential. The dotted line shows the results of Gasquess *et al.* [32], whereas the dashed-dotted line shows the results of Afanasjev *et al.* [31]. The experimental data are taken from Ref. [33].

The reaction properties govern the pathway of the evolution of stars and produce heavier elements observed in the universe.

Although the nuclear astrophysical process occurs at very high temperature, the Gamow energy, which is the most effective energy where the reaction mostly occurs, is still very low. For example, the temperature for the carbon to burn ranges from 0.8 to 1.2 GK, corresponding to the center-of-mass energies from 1 to 3 MeV. However, the Gamow energy is only around $E_G = 1.5 \pm 0.3$ MeV with the Coulomb barrier height for the $^{12}C + ^{12}C$ system at around 6.3 MeV. In this region, the cross sections are extremely small, which in many cases are not yet experimentally accessible.

Therefore, the astrophysical S factor has been introduced, which is a slowly varying function over a certain energy range and can be extrapolated to very low energies at astrophysical interest. However, for systems involved in this work, the interaction radius of the two heavy ions and the energy involved are so large that a factor gE should be introduced in order to make the S factor more plateau-like. Hence, the modified form of S factor is introduced and can be written as

$$S^*(E) = S(E)\exp(-gE), \tag{16}$$

with the units of $S^*(E)$ in MeV barns, and $S(E)$ is the normal S factor given by $S(E) = \sigma(E)E\exp(2\pi\eta)$. The factor in the exponential term, $2\pi\eta = 0.9896 Z_1 Z_2 (\mu/E)^{1/2}$, corresponds to the energy dependence of the penetration of a Coulomb barrier while $g = 0.46\ \mathrm{MeV}^{-1}$ [30] is the correction term added to the normal S factor so that $S^*(E)$ would be nearly constant at low energies.

Since the determination of fusion cross section data from the experimental measurements at very low energy is an extremely difficult task and hardly accessible, therefore the calculation of the fusion cross section in the theoretical framework is desirable in addition to the phenomenological extrapolation method of the S factor. Current work that proposes the analytical model of S factor for nonresonant reactions between heavy nuclei performed using the São Paulo potential in the frame of the barrier penetration model has been done by Afanasjev *et al.* [31]. Another analytical expression of $S(E)$ for the fusion reaction of $^{12}C + ^{12}C$ system is proposed by Gasques *et al.* [32], covering a wide energy range:

$$S(E) = 5.15 \times 10^{16} \exp\left(-0.428E - \frac{3E^{0.308}}{1 + e^{0.613(8-E)}}\right). \tag{17}$$

The $S^*(E)$ presented in Fig. 4 for $^{12}C + ^{12}C$ is calculated using Eq. (16), where $\sigma(E)$ is the calculated cross section using DFM and DFC potentials, in comparison with the analytical S factor of Afanasjev *et al.* [31] and Gasques *et al.* [32]. All the extrapolations give a good description of the average of the data in the energy range of $E = 2.5$ to 7 MeV with very small order-of-magnitude differences between A-W and the double-folding potential calculations. Only the analytical prediction from Afanasjev *et al.* [31] gives very low extrapolation of the data at very low energy. The predictions of $S^*(E)$ by different potential models are presented in Figs. 5 and 6 for $^{12}C + ^{16}O$ and $^{16}O + ^{16}O$ reactions, respectively. The figures clearly show that all the calculations are in good agreement between each other.

One important basic quantity needed for understanding the nature of stellar evolution and nucleosynthesis is the reaction rate. The astrophysical reaction rate can be calculated by using [30]

$$\langle \sigma v \rangle = \left(\frac{8}{\pi\mu}\right)^{1/2} \frac{1}{(kT)^{3/2}} \int_0^\infty \sigma(E) E \exp\left(-\frac{E}{kT}\right) dE \tag{18}$$

where the temperature T is always defined as $T_9 \times 10^9$ K.

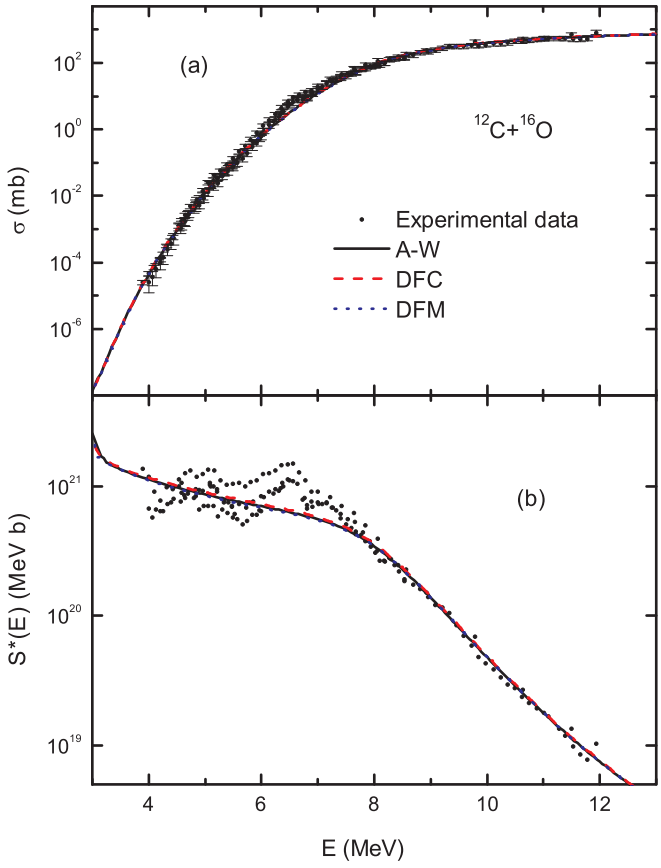

FIG. 5. (Color online) The calculated (a) cross section and (b) modified astrophysical S factor for $^{12}C + ^{16}O$ reaction. The solid and the dashed lines are the results of the calculations using the A-W and the DFC potentials, respectively, and the thick-dotted line is obtained using the DFM potential. Experimental data are taken from Ref. [34].

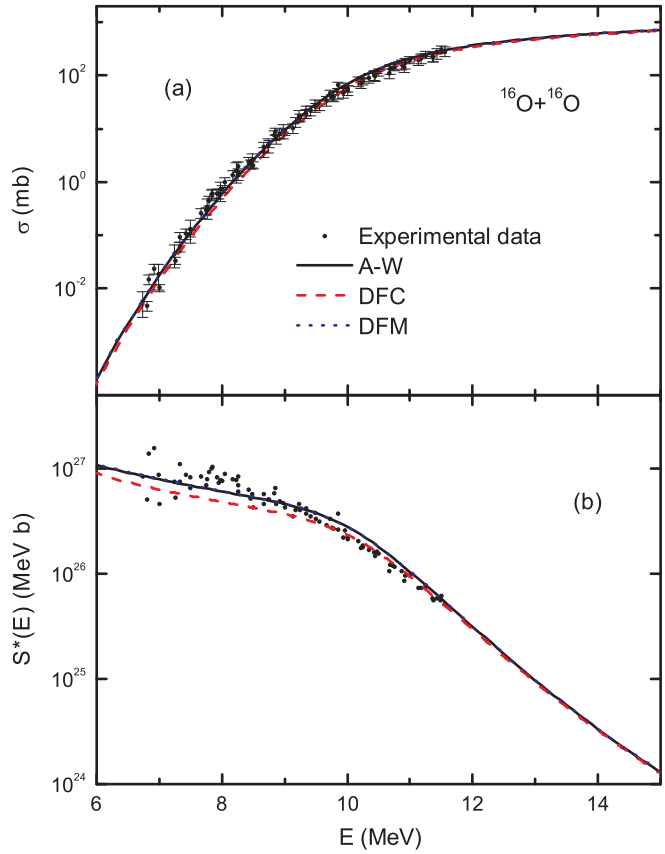

FIG. 6. (Color online) The same as for Fig. 5 but for the $^{16}O + ^{16}O$ reaction. Experimental data are taken from Ref. [35].

During the helium burning process, the core of the star contracts gravitationally, which increases the temperature and density to ignite the ^{12}C and ^{16}O ashes. Since the $^{12}C + ^{12}C$ reaction has the smallest Coulomb barrier, this reaction becomes the first to interact and therefore initiates the next burning stage, which is referred to as carbon burning. Typical temperatures in the core during carbon burning range from around 0.6 to 1.0 GK, depending on the mass of the star, while explosive carbon burning takes place in the range of 1.8 to 2.5 GK.

The calculated reaction rate from the present extrapolations for $^{12}C + ^{12}C$ reaction is depicted in Fig. 7 and is compared to the compilations of Caughlan and Fowler [36]. Obviously, the extrapolations from both double-folding potentials are in good agreement with each other but lower than the rate obtained by Caughlan and Fowler [36] at very low temperature. The straight vertical line indicates the location of the Gamow peak for temperature of the typical core carbon burning, i.e., $T \approx 0.85$ GK. It is shown that the different rates of the double-folding potentials and Caughlan and Fowler's result occur below the typical core carbon-burning temperature. The difference between the rates is about a factor of 3 to 5 at lower temperatures and slowly decreases until they are consistent with each other at higher temperatures.

The calculated reaction rate for $^{12}C + ^{16}O$ reaction, which occurs near the end of the carbon-burning phase, is presented in Fig. 8. This reaction is not expected to play a major role due

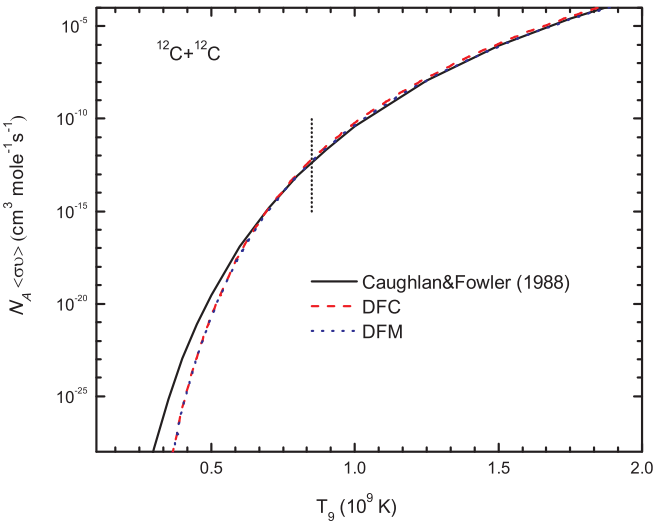

FIG. 7. (Color online) The calculated reaction rates for the fusion reaction of $^{12}C + ^{12}C$ system. The dashed and the thick-dotted lines are the results of the calculations using the DFC and DFM potentials, respectively, and the solid line is the result of Caughlan and Fowler [36].

to the larger Coulomb barrier than in the former reaction. The rate obtained from the present calculation produces the same trend as in $^{12}C + ^{12}C$ reaction.

The typical temperature for core oxygen burning is about $T \approx 2.2$ GK, with explosive oxygen burning around $T = 3.6$ GK. As expected, the reaction rates for this reaction obtained with double-folding potentials are lower than Caughlan and Fowler's at low temperature [36]. However, at the vicinity of the Gamow temperature, the rates agree with each other, as depicted in Fig. 9. The difference that mainly occurs at very low temperature is probably due to the uncertainties of the cross sections at low energy; for example, the reported cross sections for $^{12}C + ^{12}C$ reaction at energy below 3 MeV

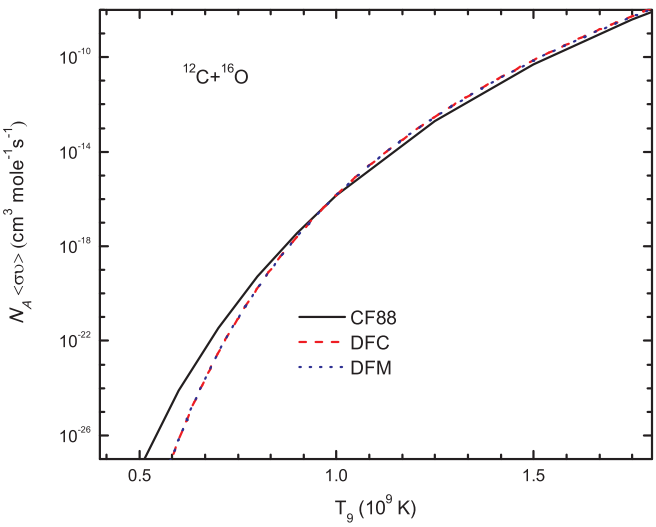

FIG. 8. (Color online) The same as in Fig. 7 but for the fusion reaction of $^{12}C + ^{16}O$ system.

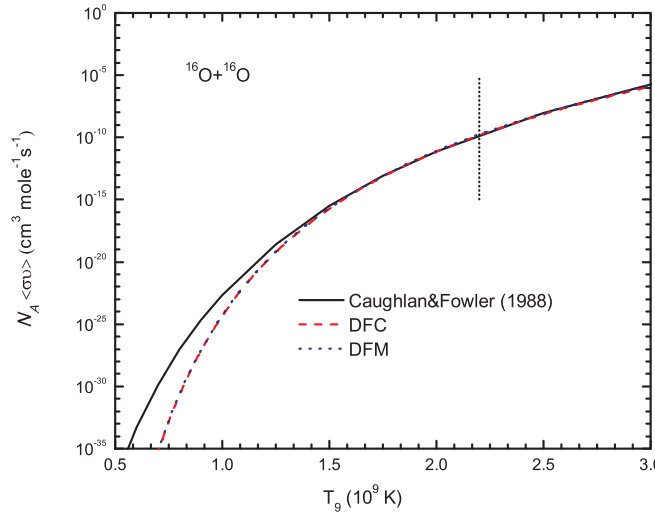

FIG. 9. (Color online) The same as for Fig. 7 but for the fusion reaction of $^{16}O + ^{16}O$ system.

are rather uncertain and show large discrepancies between different measurements [33].

V. CONCLUSION

We have studied two types of double-folding potentials, namely, the double-folding potential with zero range exchange of M3Y interaction (DFM) potential and the α-α double-folding (DFC) potential, and their applications in investigating the fusion reaction of light systems, i.e., the $^{12}C + ^{12}C$, ^{16}O, ^{24}Mg, ^{28}Si, $^{16}O + ^{16}O$, $^{24}Mg + ^{24}Mg$, ^{28}Si, and $^{28}Si + ^{28}Si$ reactions. The DFC potential seems to be less attractive and produces a higher barrier height than the DFM potential. These potentials are then used to calculate the fusion cross sections using the one-dimensional barrier penetration model. The results suggest the necessity of utilizing the normalization factor for the potential strength in order to reproduce the experimental data except for $^{12}C + ^{12}C$, ^{16}O, ^{24}Mg, and ^{28}Si reactions, where the normalization factor is unity. Overall, the fitting to the experimental data from both double-folding potentials are much better than the Akyüz-Winther potential. The value of the adjustment constant is very much dependent on the barrier height produced by the double-folding potentials.

Since the $^{12}C + ^{12}C$, ^{16}O, and $^{16}O + ^{16}O$ systems are important reactions in stellar evolution, discussion on astrophysical aspects is considered in this work. It is shown that both double-folding potentials could produce very good fitting to the extrapolation of S factor for the three astrophysical reactions. However, the calculated reaction rates obtained by these potentials are lower than the compilation of Caughlan and Fowler at low temperatures [36]. The calculation of the cross section needs to be improved in order to reduce the uncertainties in the extrapolation of the reaction rates.

Overall, in the important range of temperatures where the reactions mainly occur, the DFC potential produces very satisfactory fitting to the experimental cross section and the S-factor data. It also provides a consistent prediction of the

astrophysical reaction rates. This finding indicates that the DFC potential could be used as an alternative potential to study the reactions of light systems in the astrophysical interest.

ACKNOWLEDGMENTS

The authors are thankful to K. Hagino for useful discussion and A. A. Pharmy for giving some constructive comments. We thank the University of Malaya for Postgraduate Research Grant (PPP) No. PV089/2011A. Furthermore, A. A. Aziz acknowledges the International Islamic University Malaysia and Ministry of Education Malaysia for the Academic Training Scheme (SLAI) scholarship. N. Yusof and H. A. Kassim also acknowledge support from the University of Malaya Research Grant (UMRG) Programs No. RP006C-13AFR and No. RP012D-13AFR and University of Malaya's HIR Grant No. UM.S/625/3/HIR/28. M. Z. Firihu acknowledges support from the Directorate General for Higher Education, Ministry of Education and Culture of the Republic of Indonesia, through Fundamental Research Grant 2012.

[1] A. B. Balantekin and N. Takigawa, Rev. Mod. Phys. **70**, 77 (1998).
[2] M. Backerman, Phys. Rep. **51**, 1047 (1988).
[3] R. Vandenbosch, Annu. Rev. Nucl. Part. Sci. **42**, 447 (1992).
[4] M. Dasgupta, D. J. Hinde, N. Rowley, and A. M. Stefanini, Annu. Rev. Nucl. Part. Sci. **48**, 401 (1998).
[5] K. Hagino and N. Takigawa, Prog. Theo. Phys. **128**, 1001 (2012).
[6] O. Akyuz and A. Winter, in *Proceedings of the Enrico Fermi School of Physics, 1979*, edited by R. A. Broglia, C. H. Dasso, and R. Ricci (North Holland, Amsterdam, 1981).
[7] J. O. Newton *et al.*, Phys. Lett. B **586**, 219 (2004); J. O. Newton, R. D. Butt, M. Dasgupta, D. J. Hinde, I. I. Gontchar, C. R. Morton, and K. Hagino, Phys. Rev. C **70**, 024605 (2004).
[8] G. R. Satchler and W. G. Love, Phys. Rep. **55**, 183 (1979).
[9] G. R. Satchler, Nucl. Phys. A **329**, 233 (1979).
[10] M. L. I. Ibrahim, M. Zamrun, and H. A. Kassim, Phys. Rev. C **87**, 024611 (2013).
[11] F. M. Zamrun and K. Hagino, Phys. Rev. C **77**, 014606 (2008).
[12] F. M. Zamrun, K. Hagino, S. Mitsuoka, and H. Ikezoe, Phys. Rev. C **77**, 034604 (2008).
[13] C. L. Jiang, H. Esbensen, K. E. Rehm, B. B. Back, R. V. F. Janssens, J. A. Caggiano, P. Collon, J. Greene, A. M. Heinz, D. J. Henderson, I. Nishinaka, T. O. Pennington, and D. Seweryniak, Phys. Rev. Lett. **89**, 052701 (2002).
[14] C. L. Jiang, H. Esbensen, B. B. Back, R. V. F. Janssens, and K. E. Rehm, Phys. Rev. C **69**, 014604 (2004); C. L. Jiang *et al.*, Phys. Rev. Lett. **93**, 012701 (2004); Phys. Rev. C **71**, 044613 (2005); **73**, 014613 (2006).
[15] Ş. Mişicu and F. Carstoiu, Nucl. Phys. A **834**, 180C (2010).
[16] C. L. Jiang, K. E. Rehm, B. B. Back, and R. V. F. Janssens, Phys. Rev. C **75**, 015803 (2007).
[17] D. T. Khoa, Phys. Rev. C **63**, 034007 (2001).
[18] D. T. Khoa, W. von Oertzen, and H. G. Bohlen, Phys. Rev. C **49**, 1652 (1994).
[19] D. T. Khoa and G. R. Satchler, Nucl. Phys. A **668**, 3 (2000).
[20] I. I. Gontchar, D. J. Hinde, M. Dasgupta, and J. O. Newton, Phys. Rev. C **69**, 024610 (2004).
[21] M. E. A. Farid, Z. M. M. Mahmoud, and G. S. Hassan, Nucl. Phys. A **691**, 671 (2001).
[22] M. A. Hassanain, A. A. Ibraheem, and M. El-Azab Farid, Phys. Rev. C **77**, 034601 (2008); M. A. Hassanain *et al.*, *ibid.* **87**, 064606 (2013); M. Karakoc and I. Boztosun, *ibid.* **73**, 047601 (2006).
[23] G. Kocak, M. Karakoc, I. Boztosun, and A. B. Balantekin, Phys. Rev. C **81**, 024615 (2010).
[24] H. de Vries, C. W. de Jager, and C. de Vries, At. Data Nucl. Data Tables **36**, 495 (1987).
[25] B. Buck, H. Friedrich, and C. Wheathly, Nucl. Phys. A **275**, 246 (1977).
[26] S. Qing-biao, F. Da-chun, and Z. Yi-zhong, Phys. Rev. C **43**, 2773 (1991).
[27] O. M. Knyazkov and E. F. Hefter, Z. Phys. A **301**, 277 (1981).
[28] I. I. Gontchar and M. Chushnyakova, Comput. Phys. Commun. **181**, 168 (2010).
[29] K. Hagino *et al.* (unpublished).
[30] C. E. Rolfs and W. S. Rodney, *Cauldrons in the Cosmos* (University of Chicago Press, Chicago, 1988).
[31] A. V. Afanasjev, M. Beard, A. I. Chugunov, M. Wiescher, and D. G. Yakovlev, Phys. Rev. C **85**, 054615 (2012).
[32] L. R. Gasques *et al.*, Phys. Rev. C **72**, 025806 (2005).
[33] M. G. Mazarakis and W. E. Stephens, Phys. Rev. C **7**, 1280 (1973); E. F. Aguilera *et al.*, *ibid.* **73**, 064601 (2006); L. Barrón-Palos *et al.*, Nucl. Phys. A **779**, 318 (2006); T. Spillane *et al.*, Phys. Rev. Lett. **98**, 122501 (2007).
[34] J. R. Patterson, B. Nagorcka, G. Symons, and W. Zuk, Nucl. Phys. A **165**, 545 (1971); B. Čujec and C. A. Barnes, *ibid.* **266**, 461 (1976); P. R. Christensen, Z. E. Switkowski, and R. A. Dayers, *ibid.* **280**, 189 (1977).
[35] H. Spinka and H. Winkler, Nucl. Phys. A **233**, 456 (1974); G. Hulke, C. Rolfs, and H. P. Trautvetter, Z. Phys. A **297**, 161 (1980); S. C. Wu and C. A. Barnes, Nucl. Phys. A **422**, 373 (1984); J. Thomas, Y. T. Chen, S. Hinds, D. Meredith, and M. Olson, Phys. Rev. C **33**, 1679 (1986); A. Kuronen, J. Keinonen, and P. Tikkanen, *ibid.* **35**, 591 (1987).
[36] G. Caughlan and W. Fowler, At. Data Nucl. Data Tables **40**, 283 (1988).